Printable Materials and Devices

Rabindra N. Das, Mark D. Poliks, Frank D. Egitto and Voya R. Markovich

Research & Development, Endicott Interconnect Technologies, Inc., 1093 Clark Street, Endicott, New York, 13760.
Telephone No: 607-755-2064, E-mail: mpoliks@eitny.com

Abstract:

Printing technologies provide a simple solution to build electronic circuits on low cost flexible substrates. Materials will play an important role for developing advanced printable technology. Advanced printing is a relatively new technology and needs more characterization and optimization for practical applications. In the present paper, we examine the use of different materials in the area of printing technology. A variety of printable nanomaterials for electronic packaging have been developed. This includes nano capacitors and resistors used as embedded passives, nano laser materials, optical materials, etc. Materials can provide high capacitance densities, ranging from 5 nF/inch^2 to 25 nF/inch^2, depending on composition, particle size and film thickness. The electrical properties of capacitors fabricated from $BaTiO_3$-epoxy nanocomposites showed a stable dielectric constant and low loss over a frequency range from 1MHz to 1000MHz. Reliability of the nanocomposites was ascertained by IR-reflow, thermal cycling, pressure cooker test (PCT), and solder shock. Change in capacitance after 3X IR-reflow and after 1000 cycles of deep thermal cycling (DTC) between -55°C and 125°C was within 5%. A variety of printable discrete resistors with different sheet resistances, ranging from ohm to Mohm, processed on large panels (19.5 inches x 24 inches) have been fabricated. Low resistivity materials, with volume resistivity in the range of 10^{-4} ohm-cm to 10^{-6} ohm-cm depending on composition, particle size, and particle loading can be used as conductive joints for high frequency and high density interconnect applications. The CITC (Current Induced Thermal Cycling) life at 245C is greater than 10 cycles and life at 220C is over 25 cycles to fail, which is at least equivalent to copper PTH (plated through hole) performance. Thermosetting polymers modified with ceramics or organics can produce low k and low loss dielectrics.

Introduction:

In recent years significant progress has been achieved in the development of semiconductor packaging technology using various printing methods such as screen-printing, ink-jet printing, and microcontact printing. This trend is driven by demand for low cost, large area, flexible and lightweight devices. Since printing is inherently additive in nature, material and disposal costs are expected to be reduced, resulting in an extremely low net system cost. Most of the research activities in this printable area have been devoted to developing ink-jet solution-processable conductor materials [1-4]. Printable materials need to be chemically and physically inert to the other functional, dielectric, photoimageable materials processing in the same layer to preserve the structural and electrical integrity of devices/packages, and they have to be operationally stable to sustain long operation life. For these purposes, organic and polymeric-based materials have been widely pursued since they offer numerous advantages including low temperature processing, compatibility with organic substrates, stability over time and operation, and significant opportunity for structural modification. Nano materials/composites/hybrids provide the greatest potential benefit for high density, high speed, miniaturized advanced packaging. The small dimensions, strength, and remarkable physical and electrical properties of these structures make them very unique materials with a range of promising applications. Semiconductor devices based on functional polymers, composites, or hybrids are considered to be very promising for electronic applications since they may potentially be fabricated entirely using similar printable polymer technologies where different active fillers can be introduced within the same functional polymer system. Several nanocomposites have been reported for advanced packaging applications. Although several of these nanocomposites are not printable, the authors believe that there is room for improvement of the existing materials, so that flexible and cost effective printable materials, compatible with low temperature processes can be developed for large scale production. An effort in this direction is presented in the paper.

In this work novel printable materials that have the potential to surpass conventional materials for producing fine structures compatible with organic substrates are reported. Specifically electronic applications of printable materials (**Figure 1**) such as adhesives (both conductive and non-conductive), interlayer dielectrics (low-k, low loss dielectrics), embedded passives (capacitors, resistors), circuits, etc. are discussed. In addition, printable materials for fabrication of devices such as inductors, embedded lasers, and optical interconnects are being investigated. In the present study, epoxies are used as the typical polymer matrix, with metal /ceramic filler particles having size ranging from 10 nm to 10 microns. The addition of different fillers into the epoxy matrix controls the overall electrical properties of the composites. For example, addition of zinc oxide nano particles into epoxy shows laser like behavior upon optical pumping, and the addition of barium titanate ($BaTiO_3$) nanoparticles results in high capacitance. Thermosetting resins have advantages in terms of manufacturability, processing temperatures, low moisture absorption, high glass transition temperatures (Tg), and versatility make them quite promising for advanced packaging. However, homogeneous dispersions of ceramic particles in the epoxy matrix are a critical step in order to achieve uniform film properties.
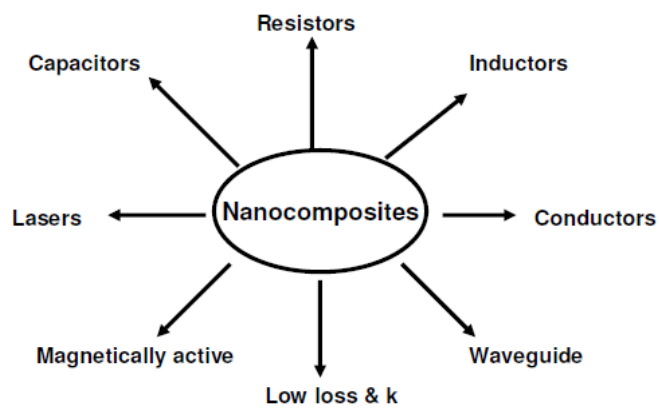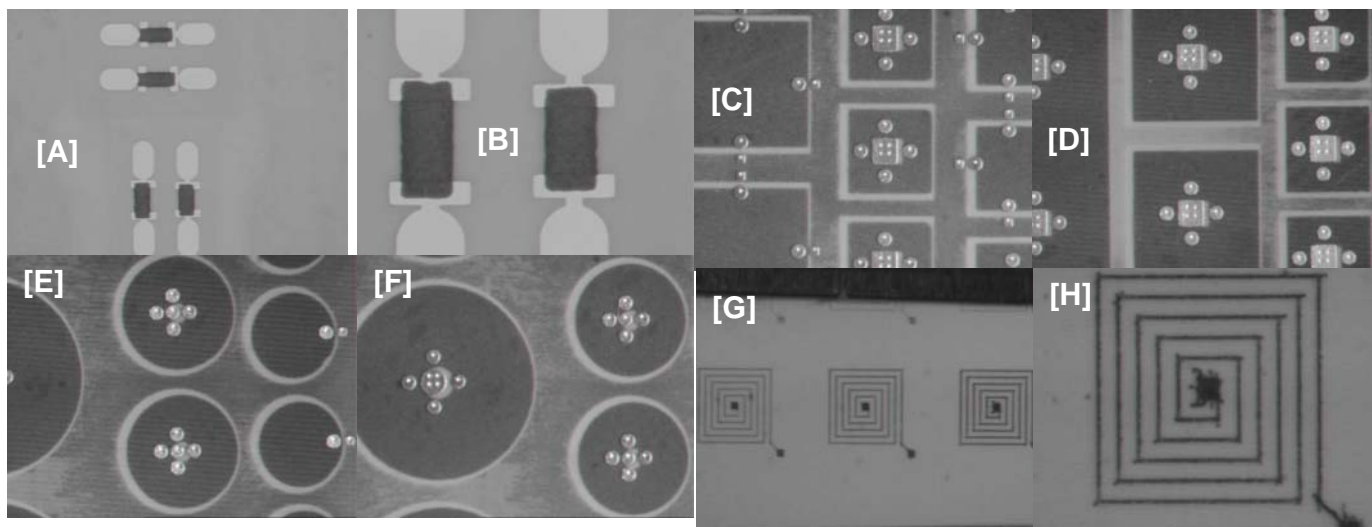
Figure 1: Overview of some of the potential applications of printable materials in microelectronics.
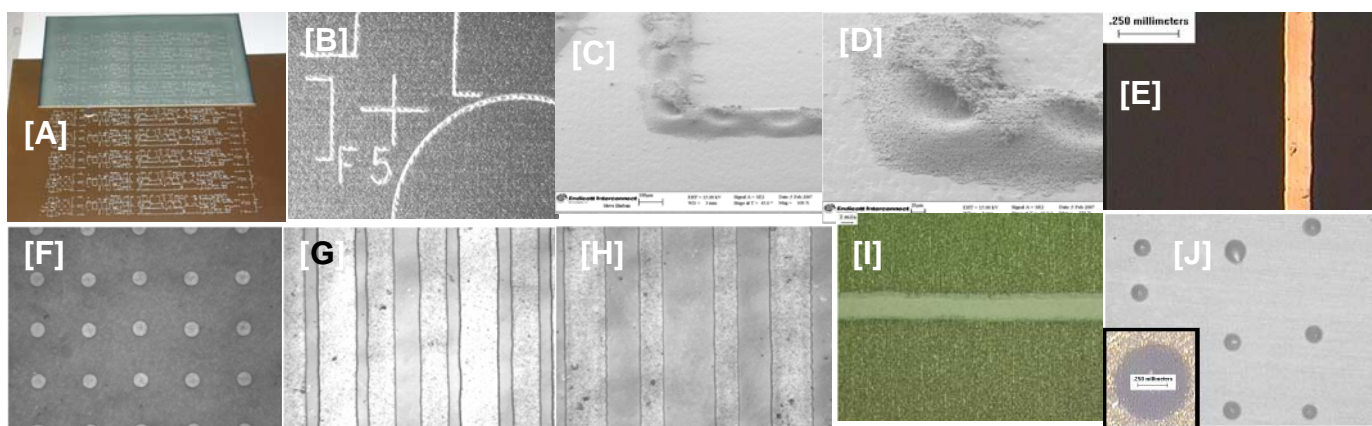
Figure 2 : Various printing process (A) Screen Print with printed area (6 inchX12 inch), (B)-(F) enlarged screen print, (G)-(H) Ink-jet print, (I) micro contact Printing, and (J) Dispensing.

Figure 3 : Various printing process (A)-(B) screen printed resistors, (C)-(F) screen printed embedded capacitors, and (G)-(H) Ink-jet printed inductors
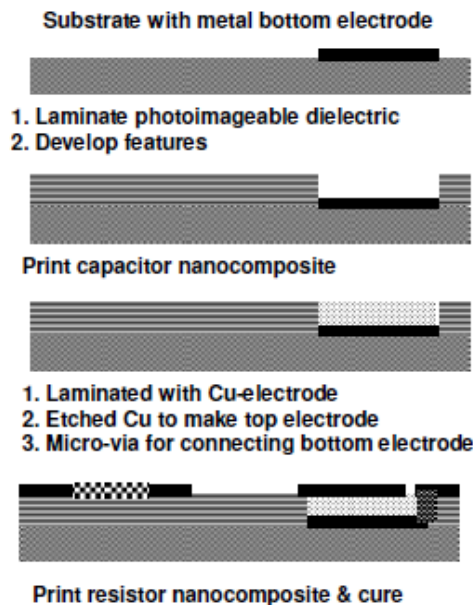
Results and Discussion:

Printable materials have potential applications at all levels of microelectronics (see **Figure 1**). This paper examines the use of nanomaterials in the area of printing technology. Printing processes have several advantages such as selective deposition, repair, and re-print capability. However, printed features with desired properties, thickness, and tolerance present significant challenges.. Nano materials concentration and corresponding viscosity is important for printing processes. Low viscosity is preferable for ink-jet printing processes, in the range of 7-10 cp. Low viscosity enables generation of submicron thin structures. Screen and contact printing are better performed using higher viscosity (100,000-150,000cp) thixotropes, and generate 10-25 micron thick features. Conducting polymers, composites, nanoparticles favor ink-jet printing for transistors and waveguides. Screen/contact printing can be used for making random lasers where surface particles are active. Embedded resistors, capacitors, and conducting circuit lines can use ink-jet or screen printing for different features. Dielectric features are typically large and can use any of the known print techniques. **Figure 2** shows various printed structres. **Figure 2A-D** represent screen printing processes. Screen print methods can produce line features in the range of 100 microns. **Figure 2E-H** represent ink-jet printings with minimum line feature size in the range of 30-100 microns. The space between two ink-jet printed lines can be reduced to 50 microns. In addition, we are developing flexible packages for a variety of applications. Several classes of flexible materials can be used to form high-performance flexible packaging. We are investigating screen and ink-jet printing for low cost flexible packages. **Figure 2I** represents micro contact printing with minimum feature size around 100 microns. For the dispensing technique, feature sizes depend upon the materials viscosity and corresponding needle used to dispense materials. It can dispense different shapes with minimum around 20 mils (500 microns) dot (**Figure 2J**). **Figure 3** shows optical photographs of various printed devices. **Figure 3A-B** represents screen printed resistors on a PTFE substrate.
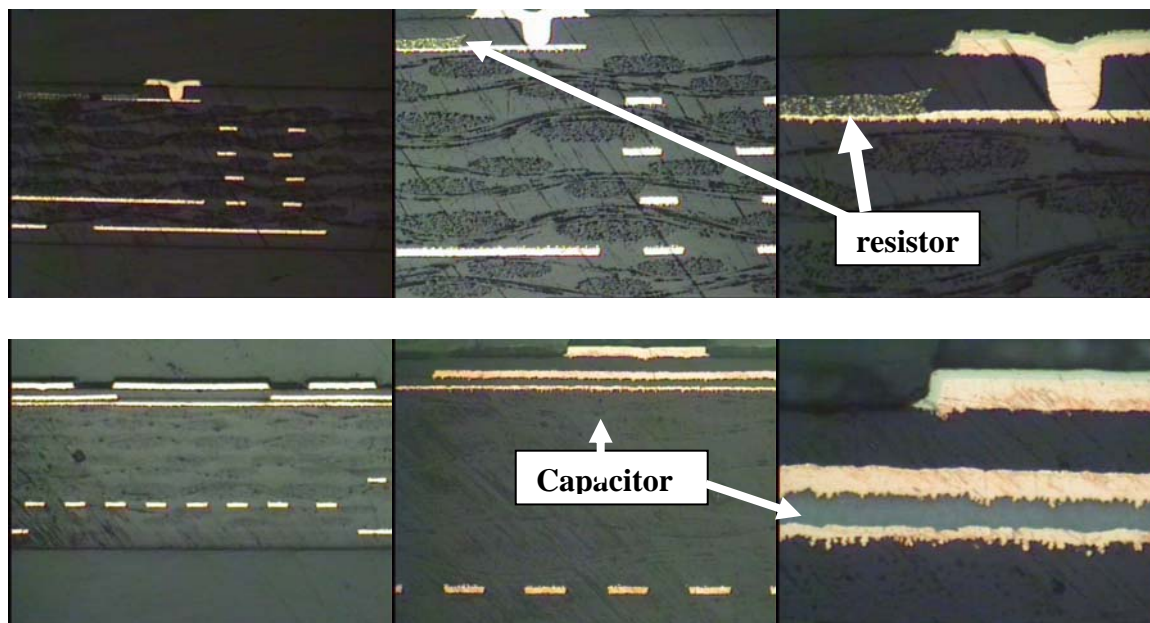
Capacitors and resistors:

A novel class of polymer nanocomposites which has shown a high dielectric constant is a $BaTiO_3$ epoxy nanocomposite. These are used to fabricate thin film embedded capacitors. High temperature/pressure lamination was used to embed capacitors in multilayer printed circuit boards. The capacitor fabrication is based on a sequential build-up technology employing a first etched Cu electrode. After patterning of the electrode, the nanocomposite can be deposited and laminated within a printed circuit board (PCB). Nanocomposites can be directly deposited by printing. **Figure 4** shows a schematic process flow for making screen printed discrete embedded capacitors and resistors. Capacitance values are defined by the feature size, thickness, and dielectric constant of the polymer-ceramic compositions. **Figure 5A** shows representative cross-sectional views of screen printed embedded capacitors and resistors. Measurement of electrical properties of capacitors fabricated from nanocomposite prints and having areas of ~2-100 mm^2 showed high capacitance density ranging from 5 nF/inch^2 to 25 nF/inch^2, depending on composition, particle size, and thickness of the prints. Thin film capacitors fabricated from 40-60% v/v $BaTiO_3$-epoxy nanocomposites showed a stable capacitance density in the range of 5-20 nF/inch^2. Capacitors fabricated from 70% v/v nanocomposite showed capacitance density of about 25 nF/inch^2.

Substrate with metal bottom electrode

1. Laminate photoimageable dielectric
2. Develop features

Print capacitor nanocomposite

1. Laminated with Cu-electrode
2. Etched Cu to make top electrode
3. Micro-via for connecting bottom electrode

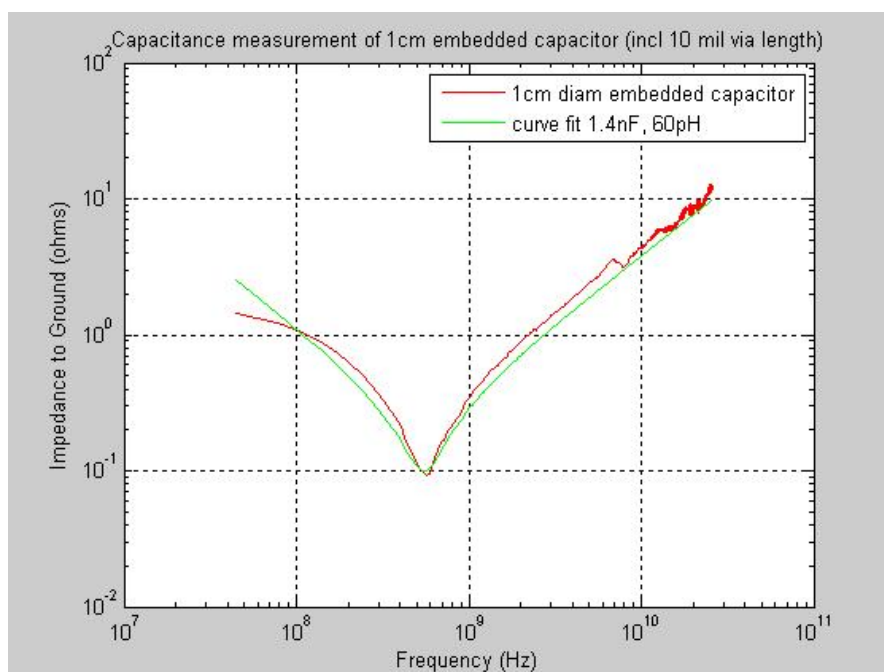Print resistor nanocomposite & cure

Figure 4: Schematic process flow for making screen printable thin film embedded capacitors and resistors.

Figure 5A: Cross-section view of screen printed embedded resistors (top) and cpacitors (bottom). Magnification is increased from left to right.


Figure 5B: Impedance profile of Capacitors.

Network Analyzer was used for high frequency measurements of printable embedded capacitors. The measurements were carried out from 45 MHz to 26GHz. **Figure 5B** shows the high frequency capacitance profile of 1 cm diameter capacitors. The curve fitting indicates that these capacitors are equivalent to a 1.4 nF bulk capacitance. The excess inductance including probe, via, and embedded capacitors was estimated to be 60 pH. **Figure 5C** shows the dielectric constant (Dk) and dissipation factor measured at 1MHz - 1000MHz for a $BaTiO_3$ epoxy nanocomposite as a representative example. Minimum Dk (3.7) and loss (0.017) was observed for pure epoxy. Addition of high dielectric constant (~1200) barium titanate particles into the epoxy matrix increases the overall dielectric constant. The dielectric properties of a nanocomposite are likely influenced in two ways: (a) by microstructure of the composite, and (b) by change in the interfacial or Maxwell's polarization at the interfaces. For a well dispersed barium titanate nanocomposite, interface polarization has a great contribution on the dielectric properties. According to Maxwell's rule for dielectric mixtures, the measured Dk (composite) values should exceed the corresponding

epoxy Dk such that Dk (epoxy) < Dk (composite) < Dk (particle). The dielectric loss increases from 0.01 to 0.025 with increasing frequency .
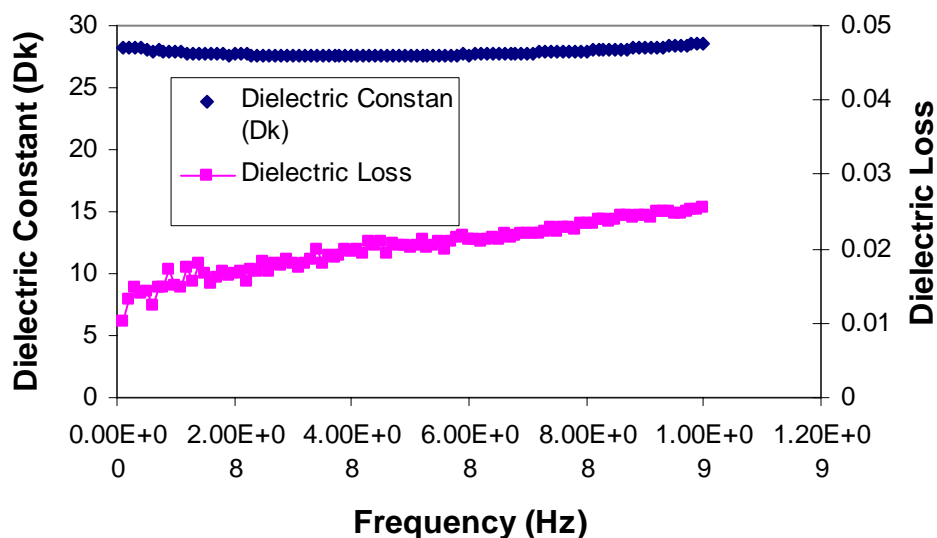
Figure 5C: Dielectric constant (Dk) and loss as a function of frequency for printable materials.

Reliability of the capacitors was ascertained by IR-reflow, thermal cycling, pressure cooker test (PCT), and solder shock. Change in capacitance after 3X IR-reflow and after 1000 cycles of deep thermal cycling (DTC) between -55°C and 125°C was within 5%. Change in capacitance after IR reflow (assembly) pre-conditioning (3X, 245 ^{o}C) and thermal shock up to 1400 cycles (-55C-125 ^{o}C) for large, medium and small embedded capacitors were less than 5% . Most of the nanocomposites in the test vehicle were stable after IR-reflow, PCT, and solder shock. Change of conductivity of electrically conducting adhesives after 3X-IR reflow at 220 ^{o}C was less than 5% (**Figure 5D**). Some of the low loss materials were also exposed to PCT (4 hrs) followed by a 15 seconds solder dip at 260 ^{o}C. In general, PCT and solder shock testing is used to induce delamination. Solder dip/shock pick will drive delamination stemming from PCT-induced defects. Initial PCT and solder dip experiments did not show any delamination. Detailed reliability testing of nanocomposites is under investigation.
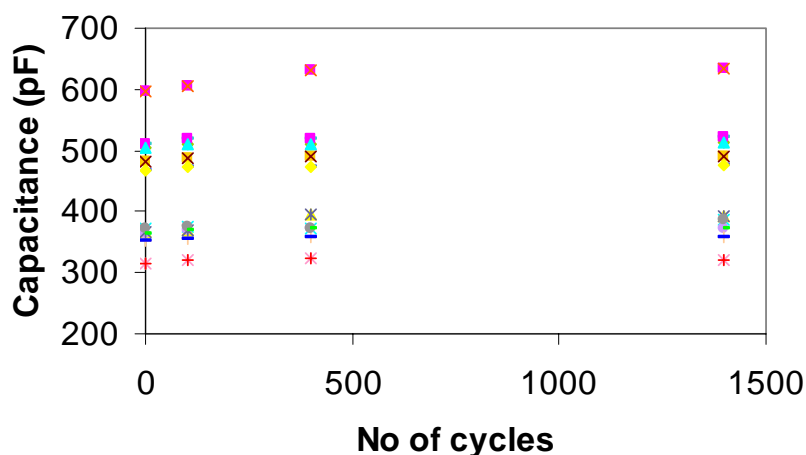

Figure 5D: Change in capacitance after IR reflow (assembly) pre-conditioning (3X, 245^{0}C) and thermal shock up to 1400 cycles (-55C-125C) for embedded capacitors

Nanocomposites are also attractive for resistor applications because variable resistor materials can be formed simply by changing the metal/insulator ratio. These compositions, however, have practical advantage only when they are capable of being printed in the internal layers of circuit boards. We have developed various discrete resistors with sheet resistance ranging from 1 ohm to 120 Mohm. Resistors in various ranges offer low temperature processing and resistor materials can be printed in the same internal layer. Representative examples of temperature profiles (25 ^{o}C -150 ^{o}C) of thin film resistors are shown in **Figure**

6. The electrical properties of resistors fabricated from epoxy nanocomposites showed a stable resistance over this temperature range.
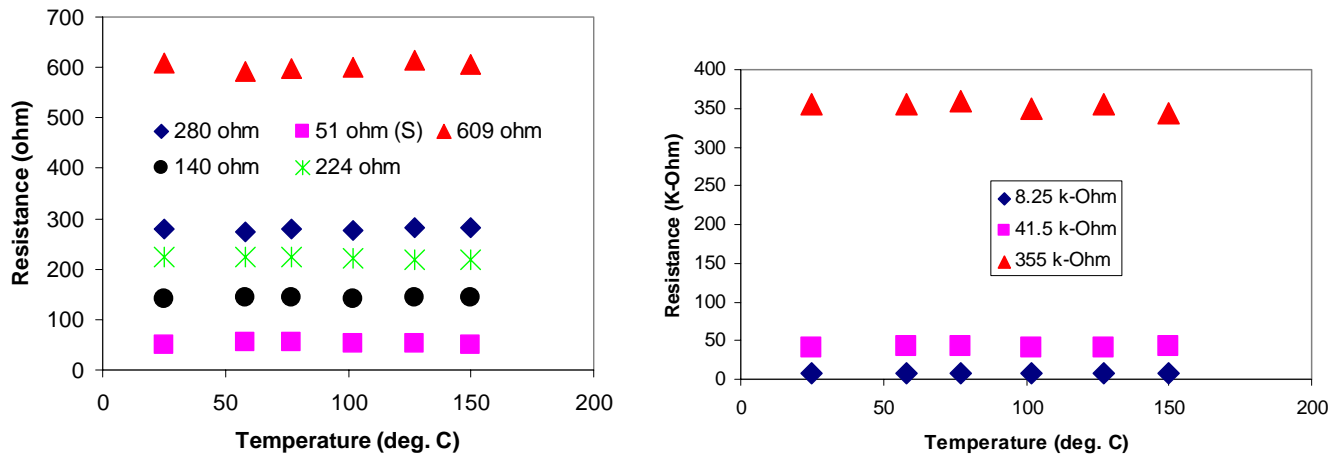

Figure 6: Change in resistance with Temperature.

Inductors:

Ink-jet printing of spiral structures can be used to form inductors. The spacing in the spiral and the resistance will dictate quality of inductors. High resistance causes thermal loss and, therefore, is not suitable for inductors. Here we have deposited multi metal layers on ink-jet printed lines to increase current carrying capacity or conductance. High conductance spirals can generate higher magnetic field at the same voltage and thus can provide higher inductance in smaller packages. We have used a variety of multi metal layers including electroless Cu, immersion gold, electroless gold, electroless palladium, electroless nickel, etc. **Figure 3G-H** shows a representative example of spiral inductors. Multi metal layer deposition on spirals reduces line resistance to hundreds of milliohms.

Conducting adhesives for interconnects:

Low resistivity nanocomposites with volume resistivity in the range of 10^{-4} ohm-cm to 10^{-6} ohm-cm, depending on composition, particle size, and loading, can be used as conductive joints for high frequency and high density interconnect applications. Metal–to-metal bonding between conductive fillers provides electrical conductivity, whereas a polymer resin provides better processability and mechanical robustness. Materials can be printed or filled in a joining core to fabricate Z-axis interconnections in laminates. Conductive joints were formed during composite lamination using an electrically conductive adhesive. The adhesive-filled joining cores were laminated with circuitized subcomposites to produce a composite structure. High temperature/pressure lamination was used to cure the adhesive in the composite and provide interconnection among the circuitized subcomposites. **Fig. 7A** shows an optical photograph of a cross section of a PWB constructed using glass-cloth reinforced dielectric materials. The construction was assembled from multiple multi-layer sub-composites. The inset shows a somewhat enlarged view of a land-to-land adhesive connection.
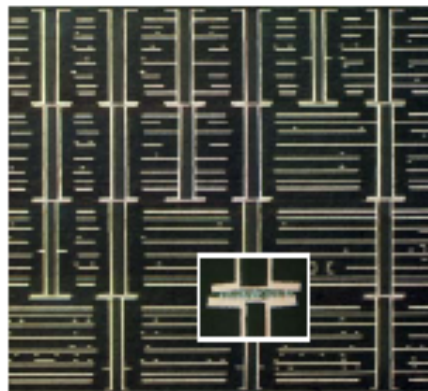

Figure 7A: Photograph of z-interconnect laminate shown in cross section.

CITC test for Z-interconnects: Z-joints are of little value in electronic packaging unless they can survive the rigors of thermal cycling, including product qualification testing, operational on/off cycles, and perhaps the most critical thermal cycle, which is the assembly reflow cycle, required to populate board before any other use. To test the reliability of joints formed using conductive materials, a Test Vehicle (TV) with Z-interconnect was fabricated. Coupons on the TV are tested with the Current Induced Thermal Cycling (CITC) test run primarily at reflow temperatures for the most rapid assessment of relative via life and failure modes, though any temperature cycle in the range of -55 to 300C is achievable with CITC. The tester uses proportional control algorithms to continuously adjust the current for each coupon in each cycle in order to achieve a precise and repeatable temperature cycle with a prescribed linear ramp and dwell time. The typical ramp rate, as used for all the data in this paper, is 3 degrees/second with a high temperature dwell time of 40 seconds, which has been shown by modeling and measurements to be sufficient to achieve thermal equilibrium [**5**]. Fans are then turned on to start the cooling phase. **Figure 7B** shows some CITC test data at both 23-220C and 23-245C. The CITC life at 245C is greater than 10 cycles and life at 220C is over 25 cycles to fail, which is excellent "copper-like" performance. In fact, failure analysis of the select coupons confirms that the final failure mode is in the copper vias, not in the Z-interconnect. That is, when processed correctly the Z interconnect can outlast the via to which it is connected. More detailed Pb-free CITC testing of Z-interconnects is under investigation.
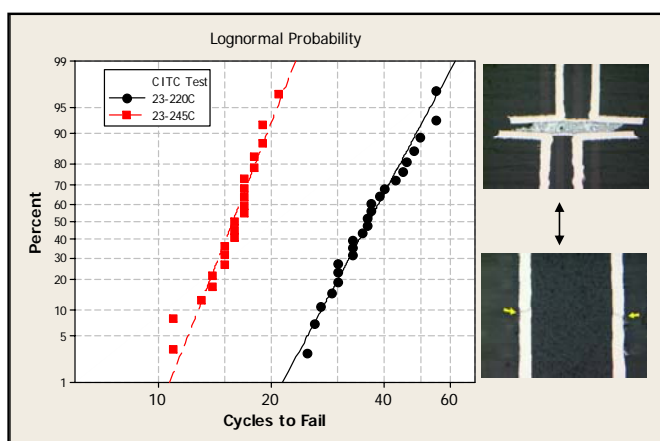
Figure 7B: CITC Cycles to fail at 23-220C and 23-245C ("Pb free") reflow temperatures for a high aspect ratio Pb free Z-interconnect product. Selected failure analysis of the earliest fails shows that the failure mode is typically a crack in the copper plated buried via, not in the Z interconnect—i.e., the lead free Z interconnect outlasted the copper buried vias to which they were joined.
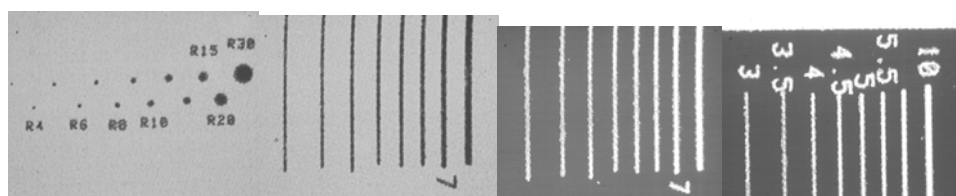

Figure 8: Printable Zinc Oxide nanocomposites

Printable ZnO:

ZnO has been proposed as an interesting material for optical devices in the blue to ultraviolet wavelength region because of its large direct bandgap of 3.4 eV. ZnO-based semiconductors can cover nearly the same wavelength range as GaN. The excitonic binding energy of ZnO is much larger than GaN-based compounds. Much attention has been given to ZnO scattered systems that, upon pumping, exhibit laser-like emission described by the term "random laser." A number of ZnO based random lasers, including ZnO polycrystalline film, powders [**6**], ZnO microlasers [**7**], ZnO based hybrids[**8**] etc., have been developed. In conventional lasers, photons reflected back and forth through a cavity stimulate the emission of more photons thereby helping to build up an intense coherent radiation beam [**9**]. A similar effect can be produced in a disordered medium containing semiconductor particles or in a finely ground semiconductor powder. If the particles or grains are close enough – less than the wavelength of light – the photons form closed loops. As a result, the light is scattered passing through the same grains, just as in an ordinary laser, light bounces back and forth between the mirrors leading to light amplification. Wiersma [**9**] suggested several possible applications of ZnO based random lasers in a variety of new miniaturized optical devices. Das and Giannelis developed a variety of ZnO polymer nanocomposites. Epoxy, PDMS (polydimethylsiloxane), and PMMA (polymethylmethacrylate) based ZnO nanocomposites show lasing at around 385 nm (blue-violet region). When ZnO is dispersed in a fluorescent polymer like poly[2-methoxy-5-(2'-ethylhexyloxy)-*p*-phenylene vinylene](MEH-PPV), it shows lasing at around 610 nm (red region). Furthermore, Zinc oxide is useful as piezoelectric and sensor materials. This material can be used as filler for capacitance layers

where ZnO improves microstructure and film quality of barium titanate epoxy capacitors. The authors have developed printable ZnO for a variety of fine structures (**Figure 8**), and can print different line widths and spacings ranging from about 3.5 - 10 mils. Smaller features, such as ~2 mil dots, can also be printed. All these features can be used as random lasers, or capacitance, or optical shielding layers. Thus, it is possible to use printable ZnO as multifunctional materials for devices.
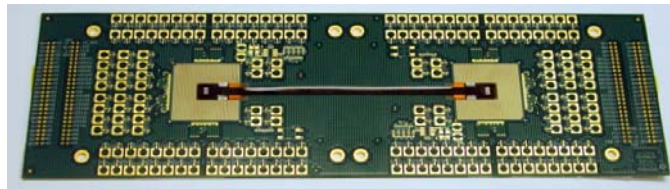
(A)
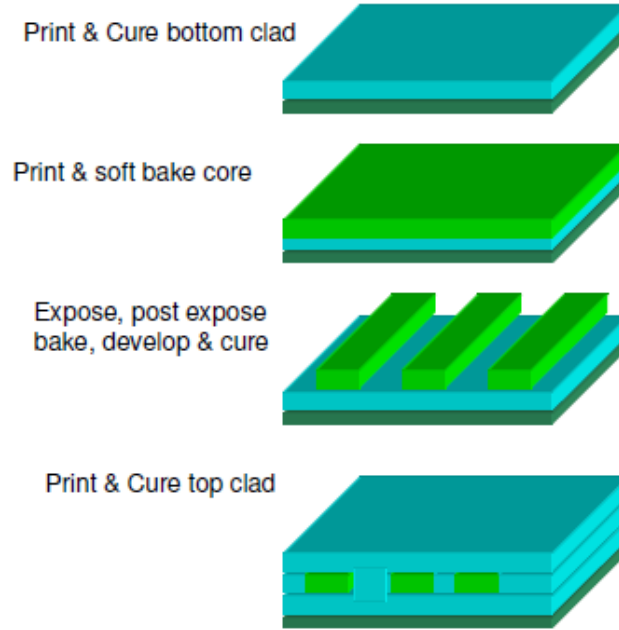
(B)

(C)

Figure 9: (A) Schematic process flow for making printable waveguides, (B) optical photo, in cross section, of optical waveguides on a 65 μm pitch, and (C) Flexible waveguide attached to the board.

Optical Waveguides:

Waveguides are important for high speed applications. Several polymers and nanocomposites are reported to be useful as waveguides. Zhang et al. [**10**], reported silver nanoparticle and rhodamine B based planar polymer multi-model waveguides. Silver nanoparticle concentration enhances the optical properties (fluorescence) of rhodamine-doped PMMA planar waveguides. Saj et al.[**11**], described plasmon waveguides composed of silver nanoplates arranged in several geometries to find the one with the lowest attenuation. They have investigated light propagation of 500-nm wavelength along different chains of silver nanoplates of sub-wavelength length and width and wavelength-size height. Yeo et al.[**12**], developed a new polymer-silica hybrid thermo-optic switch with significantly reduced crosstalk. The top cladding and the core layers are composed of polymer, while the bottom cladding layer is made of silica. Among various techniques, UV curing, micro-molding and replication are successful processes to fabricate polymer waveguides. The polymer waveguides depicted in **Figure 9B** were fabricated using an inkjet process-compatible optical polymer. Due to spatial resolution and drop size limitations of current inkjet equipment, waveguide channels cannot be "inkjet printed". Instead high resolution lithographic processes must be used to define the actual waveguide channels. Although screening of the waveguide materials is possible, inkjet processes provide excellent material deposition and coating both in terms of flexibility, with accurate and uniform thickness control in the range of two to three

microns. We have used contact and non-contact photolithographic processis with high quality photomasks for defining waveguide channels. **Figure 9A** shows a schematic process flow for making optical waveguides. Good quality waveguides with low loss (approximately 0.05dB/cm) at 850nm can be fabricated with ink-jet printing. The major challenge of deploying this technology is in the formulation of the optical polymer with suitable viscosity and adhesion properties. The flexible waveguide was attached to a PCB to produce a fully assembled optoboard. A photograph of a fully assembled optoboard is shown in **Figure 9C**.

Low K and Low Loss composites:

Low loss materials are important for high frequency and high speed applications. Low k materials are useful to reduce the dielectric thickness of the resulting circuit substrate. The rapidly growing wireless industry requires high performance materials to build low loss, high density, thermally stable integrated packages. GHz operating frequency systems require substrate materials with lower loss (Df), low dielectric constant (Dk) and good power handling characteristics, which are important in many of these applications. Low loss is a critical requirement for lightweight portable devices for long battery life. Low-k dielectrics not only lower line-to-line capacitance, but also reduce cross-talk problems between traces. Organic polymers such as divinyl siloxane benzocyclobutene (DVS-BCB), a silicon-based polymer with high organic content and poly(arylene)ethers (PAE) are some examples of low K materials. Fluoropolymers, fluorinated polyimides, polyimide-silica hybrid, and bismaleimide-triazine in combination with epoxies have been used as low loss and low k dielectric materials. The authors have studied ceramic or organic filled polymer systems where ceramic/organic fillers and content dictate the property of composites. Pure silica and muti-component silica, boron nitride, alumina and several other low k and loss fillers were used as printable composites. **Figure 10** shows variation of dielectric constant and loss with frequency. Dielectric constant decreases with increasing frequency. Screen printing and dispensing techniques are generally used for printing dielectric materials.
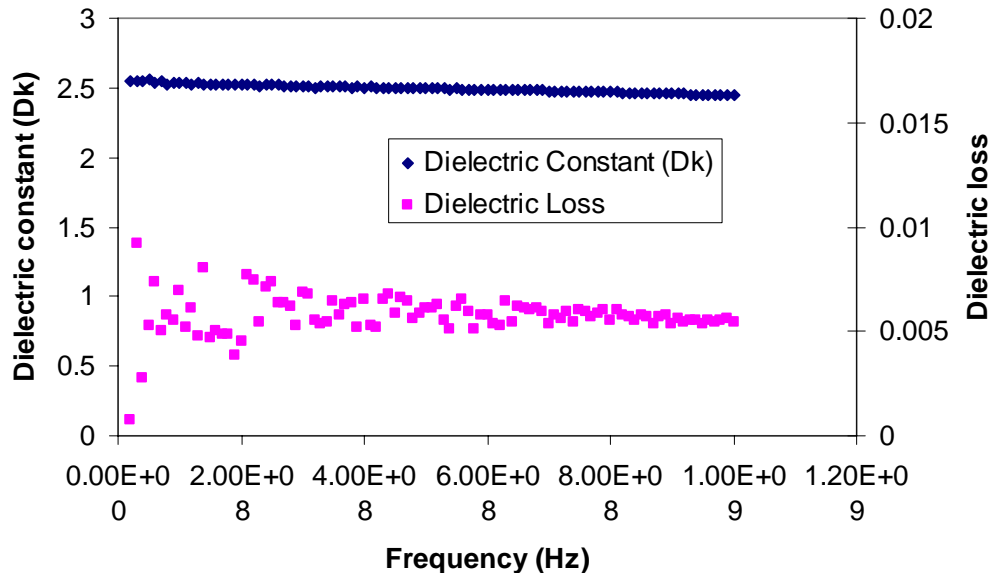
Figure 10: Dielectric constant and loss as a function of frequency for epoxy filled system.

Pb-free assembly paste:

Tin-lead solder has been widely used as an interconnection material in electronic packaging due to its low melting temperatures, good wetting behavior on various metal surface finishes, and excellent mechanical and electrical properties. As an alternative to tin-lead solder for interconnects between the die and substrate, electrically conductive adhesives (ECA) having a variety of metals within a polymeric matrix have been used. The metal fillers are loaded into the matrix in the range of 75% to 90% by weight and can include Cu, Ag and low melting point (LMP) particles.

The authors have investigated low melting filler based ECAs which can be fused to achieve metallurgical bonding between adjacent particles and between the particles and contact surfaces (solder bump and pad). It is necessary to selectively deposit ECA on the substrate pad surface using stencil printing. The interconnect between die bump and substrate pad is completed by thermal or reflow curing of the ECA. A photograph of an ECA joint structure is shown in the cross section of **Figure 11**.

The study also investigated the Flip Chip Tensile Pull Test Method to determine the fracture mode and strength of the solder bump interconnection between the flip chip die and the substrate. Chip pull strength ranges from 90-100lbs. Interconnection was

stable and failure analysis showed separation of Cu pad to substrate which is typical of pure tin-lead solder joints for the same substrate.
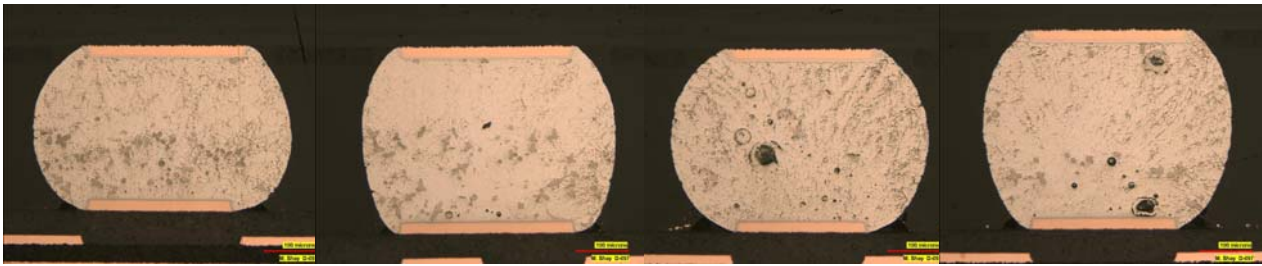
Figure 11: Photograph of paste joint shown in cross section.

Conclusions:

     Printable materials are promising not only because they are versatile, but also economical compared to other methods. A variety of materials suitable in printable processes for the fabrication of selective and localized embedded components in PWB/LCC has been developed. The materials and processes enable fine feature sizes and controlled thickness of deposited layers. This result is accomplished by using ink-jet, screening, and contact printing and dispensing processes. Experiments demonstrated that ink-jet printing and subsequent metal layer deposition is suitable for inductors, whereas screen or contact printing is suitable for conducting adhesives for interconnect applications. Capacitors, resistors, and waveguide materials can use either ink-jet or screen/contact print processes based on their requirements and viscosity of solutions. Capacitors fabricated using a printing process showed high capacitance and low loss, and are reliable after IR-Reflow and DTC. Nanomaterials can produce variable resistance ranging from ohm to Mohm. Low k and loss materials can also be fabricated from nanocomposites. Printable materials were used to provide stable, reliable z-interconnections among the circuitized subcomposites. The CITC life of Z-interconnects at 245C is greater than 10 cycles and life at 220C is over 25 cycles to fail, which is excellent "copper-like" performance. Pb-free paste was also formulated and used as an alternate approach for low temperature Pb-free assembly process. Overall, printable materials will be useful to produce multi-functional complex electronic packaging. The results also suggest that printable nanomaterials may be attractive for roll-to-roll manufacturing of large-area microelectronics such as roll-up displays, e-papers, keyboards, radiofrequency structures, transistors, photovoltaics, medical devices etc.

References:

1. G.B. Blanchet, C. R. Fincher, and F. Gao, "Polyaniline nanotube composites: A high-resolution printable conductor" Appl. Phys. Lett., Vol. 82, No. 8, 1291.
2. D. Huang, F. Liao, S. Molesa, D. Redinger, and V. Subramanian, "Plastic-Compatible Low Resistance Printable Gold Nanoparticle Conductors for Flexible Electronics" *Journal of The Electrochemical Society*, 150 (7) G412-G417 (2003).
3. H-H Lee, K-S Chou, K-C Huang, "Inkjet printing of nanosized silver colloids" Nanotechnology 16 (2005) 2436–2441.
4. Yiliang Wu, Yuning Li, Ping Liu, Sandra Gardner, and Beng S. Ong, "Studies of Gold Nanoparticles as Precursors to Printed Conductive Features for Thin-Film Transistors" *Chem. Mater.* 2006, *18,* 4627-4632.
5. Kevin Knadle "Reliability and Failure Mechanisms of Laminate Substrates in a Pb-free World" IPC APEX 2009, Las Vegas, NV March 2009.
6. I. Ozerov, M. Arab, V. I. Safarov, W. Marine, S. Giorgio, M. Sentis, L. Nanai, *"Enhancement of exciton emission from ZnO nanocrystalline films by pulsed laser annealing"* Appl. Surf. Sci., 226 (2004) 242.
7. Y. Ling, H. Cao, A. L. Burin, M. A. Ratner, X. Liu, R. P. H. Chang, *"Investigation of random lasers with resonant feedback"* Phys. Rev. A, 64 (2001) 063808.
8. G. van Soest, M. Tomita, A. Lagendijk, *"Amplifying volume in scattering media"* Opt. Lett., 24 (1999) 306.
9. D. Wiersma, Nature, 406, 132 (2000).
10. D-G Zhang, P. Wang, X-J Jiao, X-H Sun, D-M Liu, "Fluorescence enhancement of a polymer planer waveguide doped with Rhodamine B and silver nanoparticles." Chin. Phys. Lett. 23(10)2848(2006).
11. W.M. Saj, T.J. Antosiewicz, J. Pniewski, and T. Szoplik, " Energy transport in Plasmon waveguides on chains of metal nanoparticles" Opto-Elecetronic Review 4(3)243-251(2006).
12. Dong-Min Yeo , Sang-Yung Shin, "Polymer-silica hybrid 1 · 2 thermooptic switch with low crosstalk" Optics Communications 267 (2006) 388–393.